UNIVERSITYOF BIRMINGHAM

University of Birmingham
Research at Birmingham

Early Advanced LIGO binary neutron-star sky localization and parameter estimation

Berry, C P L; Farr, B; Farr, W M; Haster, C-J; Mandel, I; Middleton, H; Singer, L P; Urban, A L; Vecchio, A; Vitale, S; Cannon, K; Graff, P B; Hanna, Chad; Mohapatra, S; Pankow, C; Price, L R; Sidery, T; Veitch, J

Document Version
Publisher's PDF, also known as Version of record

Link to publication on Research at Birmingham portal

Download date: 09. May. 2024

PAPER • OPEN ACCESS

Early Advanced LIGO binary neutron-star sky localization and parameter estimation

To cite this article: C P L Berry et al 2016 *J. Phys.: Conf. Ser.* **716** 012031

View the article online for updates and enhancements.

IOP ebooks™

Bringing you innovative digital publishing with leading voices to create your essential collection of books in STEM research.

Start exploring the collection - download the first chapter of every title for free.

Early Advanced LIGO binary neutron-star sky localization and parameter estimation

C P L Berry[1], B Farr[2], W M Farr[1], C-J Haster[1], I Mandel[1], H Middleton[1], L P Singer[3], A L Urban[4], A Vecchio[1], S Vitale[5], K Cannon[6], P B Graff[7,8], C Hanna[9,10], S Mohapatra[5,11], C Pankow[4], L R Price[12], T Sidery[1] and J Veitch[1]

[1] School of Physics & Astronomy, University of Birmingham, Birmingham, B15 2TT, UK

[2] Enrico Fermi Institute, University of Chicago, Chicago, IL 60637, USA

[3] Astrophysics Science Division, NASA Goddard Space Flight Center, Greenbelt, MD 20771, USA

[4] Leonard E. Parker Center for Gravitation, Cosmology, and Astrophysics, University of Wisconsin–Milwaukee, Milwaukee, WI 53201, USA

[5] Massachusetts Institute of Technology, 185 Albany St, Cambridge, MA 02139, USA

[6] Canadian Institute for Theoretical Astrophysics, 60 St. George Street, University of Toronto, Toronto, Ontario, M5S 3H8, Canada

[7] Department of Physics, University of Maryland–College Park, College Park, MD 20742, USA

[8] Gravitational Astrophysics Lab, NASA Goddard Space Flight Center, Greenbelt, MD 20771, USA

[9] Perimeter Institute for Theoretical Physics, Ontario, N2L 2Y5, Canada

[10] Pennsylvania State University, University Park, PA 16802, USA

[11] Syracuse University, Syracuse, NY 13244, USA

[12] LIGO Laboratory, California Institute of Technology, Pasadena, CA 91125, USA

E-mail: `cplb@star.sr.bham.ac.uk`

Abstract. 2015 will see the first observations of Advanced LIGO and the start of the gravitational-wave (GW) advanced-detector era. One of the most promising sources for ground-based GW detectors are binary neutron-star (BNS) coalescences. In order to use any detections for astrophysics, we must understand the capabilities of our parameter-estimation analysis. By simulating the GWs from an astrophysically motivated population of BNSs, we examine the accuracy of parameter inferences in the early advanced-detector era. We find that sky location, which is important for electromagnetic follow-up, can be determined rapidly (~ 5 s), but that sky areas may be hundreds of square degrees. The degeneracy between component mass and spin means there is significant uncertainty for measurements of the individual masses and spins; however, the chirp mass is well measured (typically better than 0.1%).

1. Introduction

The advanced generation of ground-based gravitational-wave (GW) detectors, Advanced LIGO (aLIGO) [1] and Advanced Virgo (AdV) [2], begin operation soon: the first observing run (O1) of aLIGO is September 2015–January 2016 [3]. Binary neutron stars (BNSs) are a promising source [4].[1]

---

[1] Since submission, the first detection (of a binary black hole rather than a BNS), has been announced [5].

Analysis of a signal goes through several stages: detection, low-latency parameter estimation (PE), mid-latency PE and high-latency PE [6]. Each refines our understanding. To discover what we can learn about BNSs, a simulated astrophysically motivated population of BNS signals (component masses $m_{1,2} \in [1.2, 1.6]M_\odot$, isotropic spins with magnitudes $a_{1,2} \in [0, 0.05]$, and uniformly distributed in volume [7]) has been studied in an end-to-end analysis, with results reported in several publications. Singer *et al.* [7] studied the (low- and mid-latency) prospects for sky localization.[2] Berry *et al.* [8] repeated the analysis using more realistic noise (detector noise from the sixth science run of initial LIGO [9] recoloured to match the expected sensitivity of early aLIGO [10]), in contrast to ideal Gaussian noise. In addition to considering sky localization, Berry *et al.* [8] also investigated measurements of source distance and mass. The latter is influenced by spin, Farr *et al.* [11] completed the high-latency analysis including the effects of spin, considering all aspects of PE. We report results from these studies for O1 PE; further technical details are in the papers themselves.

2. Sky localization
Sky localization can be computed at low-latency by BAYESTAR [12] or at mid- to high-latency by LALINFERENCE [13].[3] Both are fully Bayesian PE codes; BAYESTAR uses the output of the detection pipeline, while LALINFERENCE matches GW templates to the measured detector strain [14]. Computing templates is computationally expensive; mid-latency PE is done with (non-spinning) TaylorF2 and high-latency PE is done with (fully spin-precessing) SpinTaylorT4. Both are inspiral-only post-Newtonian waveforms [15]. BAYESTAR takes a median time of 4.5 s to calculate the location [12]; the median times for the non-spinning and spinning LALINFERENCE analyses to collect 2000 posterior samples are $\sim 5.7 \times 10^4$ s [8] and $\sim 9.2 \times 10^5$ s [11] respectively.

Despite their differences, BAYESTAR and LALINFERENCE produce consistent results for a two-detector network.[4] The inclusion of spin in PE does not change sky localization for this slowly spinning population (the same may not be true for rapidly spinning black holes). At a constant signal-to-noise ratio (SNR) ϱ, there is also a negligible difference between results from Gaussian and recoloured noise. The scaling of the 50% credible region $CR_{0.5}$ and 90% credible region $CR_{0.9}$ with SNR is shown in Fig. 1. Assuming a detection threshold of a false alarm rate of 10^{-2} yr^{-1} ($\varrho \gtrsim 10$–12), the median $CR_{0.5}$ ($CR_{0.9}$) is 170 deg^2 (690 deg^2) using BAYESTAR and 150 deg^2 (630 deg^2) using LALINFERENCE; switching to a threshold of $\varrho \geq 12$ [3], these become 140 deg^2 (520 deg^2) and 120 deg^2 (480 deg^2) respectively [8].

3. Mass and spin
The first estimates for the component masses $m_{1,2}$ come from the detection pipeline, here GSTLAL [16]. Full posteriors are constructed by LALINFERENCE. The degeneracy between mass and spin complicates measurements. Excluding spins (as in the mid-latency analysis) means we can miss the true parameter values. Allowing spins to vary over the full (black hole) range of $a_{1,2} \in [0, 1]$ (as in the high-latency analysis) and including precession ensures we cover the true value, but potentially means that we consider spin values not found in nature: here, the spins are $a_{1,2} < 0.05$, but we will not know the true distribution in practice.

The chirp mass $\mathcal{M} = (m_1 m_2)^{3/5}/(m_1 + m_2)^{1/5}$ is the best measured mass parameter. Fig. 2(a) shows the offset between chirp-mass estimates (maximum likelihood values for GSTLAL and posterior means for LALINFERENCE) and the true values. All methods produce accurate results (offsets $< 0.5\%$) and there is no noticeable difference between recoloured and Gaussian noise. The mid-latency offsets are smaller than the high-latency ones, because our BNSs are slowly

---

[2] Singer *et al.* [7] also considered the second observing run (O2), with AdV joining the network.
[3] Part of the LIGO Algorithm Library (LAL) available from www.lsc-group.phys.uwm.edu/lal.
[4] This is not the case in a three-detector network if there is not a trigger from all the detectors [7, 12].

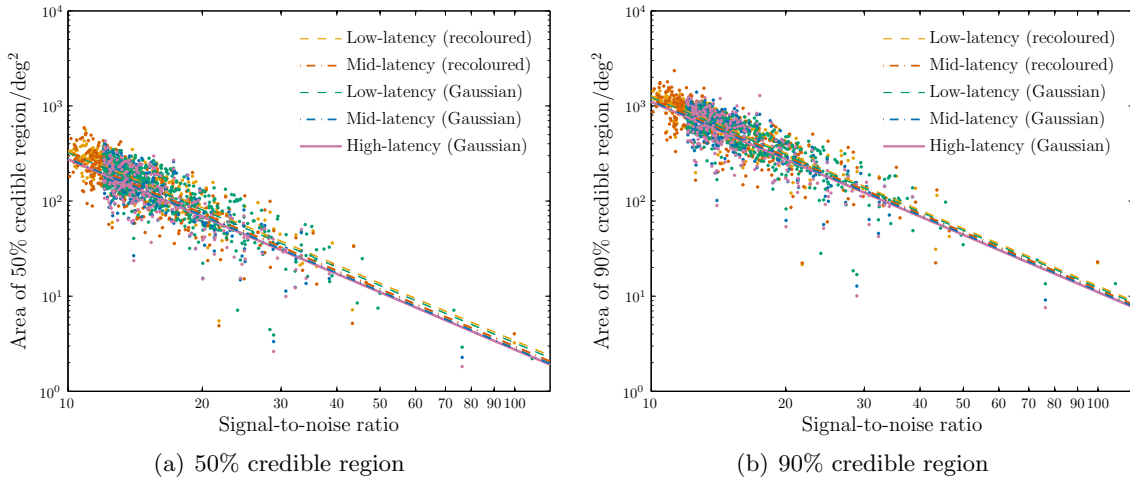(a) 50% credible region (b) 90% credible region

Figure 1. Sky localization versus SNR for the low-latency BAYESTAR, the mid-latency (non-spinning) LALINFERENCE and the high-latency (spinning) LALINFERENCE analyses [7, 8, 11]. Individual results are indicated by points and lines indicate best fits assuming $\mathrm{CR}_p \propto \varrho^{-2}$; these are $\mathrm{CR}_{0.5} \approx (2.84 \times 10^4)\varrho^{-2}$ deg^2 and $\mathrm{CR}_{0.9} \approx (1.14 \times 10^5)\varrho^{-2}$ deg^2 across the range considered.

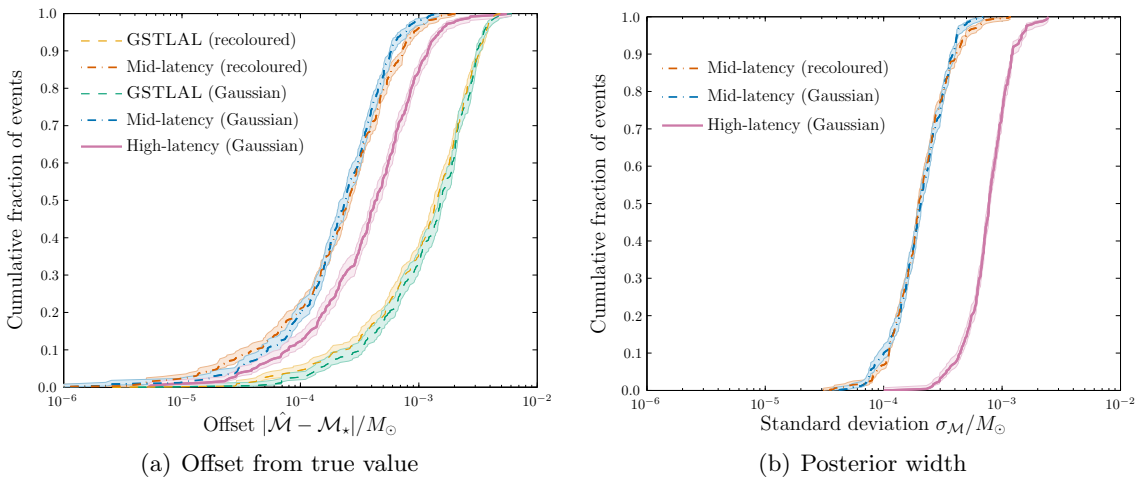(a) Offset from true value (b) Posterior width

Figure 2. Cumulative fractions of events with (a) offsets in chirp-mass estimates and (b) posterior standard deviations smaller than the abscissa value [8, 11]. The offset is the difference between the true value $\mathcal{M}_*$ and maximum likelihood value from GSTLAL or the posterior mean from (mid- or high-latency) LALINFERENCE. The shaded areas are the 68% confidence intervals on the cumulative distributions.

spinning (which need not be the case in reality). However, the mid-latency offsets are more statistically significant. The mean values of $(\hat{\mathcal{M}} - \mathcal{M})^2 / \sigma_{\mathcal{M}}^2$, where $\sigma_{\mathcal{M}}$ is the posterior standard deviation, are 5.5, 5.1 and 0.7 for the recoloured non-spinning, Gaussian non-spinning and Gaussian spinning analyses respectively. Ignoring spin yields posteriors that are too narrow [8], the distribution of $\sigma_{\mathcal{M}}$ is shown in Fig. 2(b) [11]; the median values of $\sigma_{\mathcal{M}}$ are $2.0 \times 10^{-4} M_\odot$, $2.1 \times 10^{-4} M_\odot$ and $7.7 \times 10^{-4} M_\odot$ for the recoloured non-spinning, Gaussian non-spinning and Gaussian spinning analyses respectively.

Measurements of other mass parameters, such as the mass ratio $q = m_2/m_1 \ (0 < q \leq 1)$ or

$m_{1,2}$, are less precise, and the degeneracy with spin is more pronounced [11, 14]: the median 50% (90%) credible interval for q is 0.29 (0.59). For our population of low-spin BNSs, the spins are not well measured and have large uncertainties. None of the events have a 50% upper credible bound less than 0.1; the median 50% (90%) upper credible bound is 0.30 (0.70) for a_1 (the dominant spin) and 0.42 (0.86) for a_2. Low spin values are preferred, but spin magnitudes can only be weakly constrained.

4. Summary
O1 marks the beginning of the advanced-detector era. As time progresses, sensitivities improve and further detectors (AdV, LIGO-India [17] and KAGRA [18]) come online, the prospects for detection and PE will become better [7, 19, 20]. For BNSs, chirp mass is always well measured, but sky localization and spins are more uncertain.

Acknowledgments

References
[1] Aasi J *et al* (LIGO Scientific Collaboration) 2015 *Class. Quantum Grav.* **32** 074001 (*Preprint* 1411.4547)

[2] Acernese F *et al* (Virgo Collaboration) 2015 *Class. Quantum Grav.* **32** 024001 (*Preprint* 1408.3978)

[3] Abbott B P *et al* (LIGO–Virgo Collaboration) 2016 *Living Rev. Relat.* **19** 1 (*Preprint* 1304.0670)

[4] Abadie J *et al* (LIGO–Virgo Collaboration) 2010 *Class. Quantum Grav.* **27** 173001 (*Preprint* 1003.2480)

[5] Abbott B *et al* (LIGO–Virgo Collaboration) 2016 *Phys. Rev. Lett.* **116** 061102 (*Preprint* 1602.03837)

[6] Aasi J *et al* (LIGO–Virgo Collaboration) 2014 The LSC–Virgo White Paper on Gravitational Wave Searches and Astrophysics Tech. Rep. LIGO-T1400054-v7 URL https://dcc.ligo.org/T1400054/public

[7] Singer L P *et al* 2014 *Astrophys. J.* **795** 105 (*Preprint* 1404.5623)

[8] Berry C P L *et al* 2015 *Astrophys. J.* **804** 114 (*Preprint* 1411.6934)

[9] Aasi J *et al* (LIGO–Virgo Collaboration) 2015 *Class. Quantum Grav.* **32** 115012 (*Preprint* 1410.7764)

[10] Barsotti L and Fritschel P (LIGO Scientific Collaboration) 2012 Early aligo configurations: example scenarios toward design sensitivity Tech. Rep. LIGO-T1200307-v4 URL https://dcc.ligo.org/LIGO-T1200307/public

[11] Farr B *et al* 2015 (*Preprint* 1508.05336)

[12] Singer L P and Price L R 2016 *Phys. Rev.* D **93** 024013 (*Preprint* 1508.03634)

[13] Veitch J *et al* 2015 *Phys. Rev.* D **91** 042003 (*Preprint* 1409.7215)

[14] Cutler C and Flanagan E E 1994 *Phys. Rev.* D **49** 2658–2697 (*Preprint* gr-qc/9402014)

[15] Buonanno A, Iyer B, Ochsner E, Pan Y and Sathyaprakash B S 2009 *Phys. Rev.* D **80** 084043 (*Preprint* 0907.0700)

[16] Cannon K *et al* 2012 *Astrophys. J.* **748** 136 (*Preprint* 1107.2665)

[17] Iyer B, Souradeep T, Unnikrishnan C S, Dhurandhar S, Raja S and Sengupta A (IndIGO Consortium) 2011 LIGO-India LIGO Technical Report M1100296-v2 URL https://dcc.ligo.org/LIGO-M1100296/public

[18] Aso Y, Michimura Y, Somiya K, Ando M, Miyakawa O, Sekiguchi T, Tatsumi D and Yamamoto H (KAGRA Collaboration) 2013 *Phys. Rev.* D **88** 043007 (*Preprint* 1306.6747)

[19] Schutz B F 2011 *Class. Quantum Grav.* **28** 125023 (*Preprint* 1102.5421)

[20] Veitch J *et al* 2012 *Phys. Rev.* D **85** 104045 (*Preprint* 1201.1195)